



HAL
open science

Spinal cord and brain tissue impairments as long-term effects of rugby practice? An exploratory study based on T1 and ihMTsat measures

Arash Forodighasemabadi, Guillaume Baucher, Lucas Soustelle, Thomas Troalen, Olivier Girard, Maxime Guye, Jean-Baptiste Grisoli, Jean-Philippe Ranjeva, Guillaume Duhamel, Virginie Callot

► To cite this version:

Arash Forodighasemabadi, Guillaume Baucher, Lucas Soustelle, Thomas Troalen, Olivier Girard, et al.. Spinal cord and brain tissue impairments as long-term effects of rugby practice? An exploratory study based on T1 and ihMTsat measures. *Neuroimage-Clinical*, 2022, 35, pp.103124. 10.1016/j.nicl.2022.103124 . hal-03770501

HAL Id: hal-03770501

<https://amu.hal.science/hal-03770501>

Submitted on 6 Sep 2022

HAL is a multi-disciplinary open access archive for the deposit and dissemination of scientific research documents, whether they are published or not. The documents may come from teaching and research institutions in France or abroad, or from public or private research centers.

L'archive ouverte pluridisciplinaire **HAL**, est destinée au dépôt et à la diffusion de documents scientifiques de niveau recherche, publiés ou non, émanant des établissements d'enseignement et de recherche français ou étrangers, des laboratoires publics ou privés.



Distributed under a Creative Commons Attribution - NonCommercial - NoDerivatives 4.0 International License

1 **Spinal cord and brain tissue impairments as long-term effects of rugby**
2 **practice? An exploratory study based on T₁ and ihMTsat measures.**

3
4 **Authors**

5 Arash Forodighasemabadi^{1,2,3,4}, Guillaume Baucher^{1,2,5}, Lucas Soustelle^{1,2}, Thomas Troalen⁶,
6 Olivier M. Girard^{1,2}, Maxime Guye^{1,2}, Jean-Baptiste Grisoli⁷, Jean-Philippe Ranjeva^{1,2},
7 Guillaume Duhamel^{1,2}, and Virginie Callot^{1,2,4,*}

8
9 **Affiliations**

10 1 Aix-Marseille Univ, CNRS, CRMBM, Marseille, France

11 2 APHM, Hopital Universitaire Timone, CEMEREM, Marseille, France

12 3 Aix-Marseille Univ, Université Gustave Eiffel, LBA, Marseille, France

13 4 iLab-Spine International Associated Laboratory, Marseille-Montreal, France-Canada

14 5 APHM, Hopital Universitaire Nord, Neurosurgery Dept, Marseille, France

15 6 Siemens Healthcare SAS, Saint-Denis, France

16 7 APHM, Hopital Universitaire Timone, Pôle MPR, Marseille, France

17
18 *** Corresponding author**

19 Virginie Callot

20 CRMBM-CEMEREM, UMR 7339, CNRS - Aix-Marseille Université, Faculté de Médecine

21 27, bd Jean Moulin, 13385 Marseille Cedex 5, France.

22 virginie.callot@univ-amu.fr

23 Tel: +33491388465

24
25 **CRedit roles**

26
27 Arash Forodighasemabadi: Conceptualization; Data curation; Formal analysis; Investigation;
28 Methodology; Software; Validation; Visualization; Roles/Writing - original draft; Writing -
29 review & editing

30
31 Guillaume Baucher: Formal analysis; Investigation; Methodology; Visualization; Writing -
32 review & editing

33

34 Lucas Soustelle: Formal analysis; Methodology; Software; Writing - review & editing
35
36 Thomas Troalen: Methodology; Writing - review & editing
37
38 Olivier M. Girard: Conceptualization; Formal analysis; Methodology; Validation; Writing -
39 review & editing
40
41 Maxime Guye: Project administration; Resources.
42
43 Jean-Baptiste Grisoli : Conceptualization ; Data curation ; Resources
44
45 Jean-Philippe Ranjeva: Conceptualization; Formal analysis; Validation; Writing - review &
46 editing
47
48 Guillaume Duhamel: Conceptualization; Formal analysis; Methodology; Validation ; Writing
49 - review & editing
50
51 Virginie Callot: Conceptualization; Data curation ; Formal analysis ; Funding acquisition;
52 Investigation ; Methodology ; Project administration ; Resources ; Supervision ; Validation ;
53 Visualization ; Writing - review & editing
54
55
56
57
58
59
60
61
62
63 **Abbreviations**
64 CSA: Cross-Sectional Area
65 cSC: Cervical Spinal Cord
66 CSF: Cerebrospinal Fluid
67 CST: Corticospinal Tracts

68 GM: Gray Matter
69 HC: Healthy Control
70 ihMT: inhomogeneous Magnetization Transfer
71 LST: Lateral Sensory Tracts
72 mJOA: Modified Japanese Orthopedic Association
73 MP2RAGE: Magnetization Prepared 2 Rapid Acquisition Gradient Echo
74 NDI: Neck Disability Index
75 OSS: Overall Stenosis Score
76 PST: Posterior Sensory Tracts
77 R: Rugby player
78 RST: Reticulo/Rubrospinal Tracts
79 WM: White Matter

80
81

82 **Highlights**

83
84

- 85 • Diffuse degeneration of spinal cord (higher T_1) is observed in retired rugby players
- 86
- 87 • Demyelination of brain WM tracts (higher T_1 / lower ihMTsat values) is present in
- 88 rugby players
- 89
- 90 • Early aging in both brain and spinal cord tissues may be linked to the rugby practice
- 91
- 92 • The aforementioned effects may suggest cumulative effects of long-term impacts on
- 93 the tissues

94
95

96 **Abstract**

97

98 Rugby players are subject to multiple impacts to their head and neck that could have adverse
99 neurological effects and put them at increased risk of neurodegeneration.

100 Previous studies demonstrated altered default mode network and diffusion metrics on brain,
101 as well as more foraminal stenosis, disc protrusion and neck pain among players of contact
102 sports as compared to healthy controls. However, the long-term effects of practice and
103 repetitive impacts on brain and cervical spinal cord (cSC) of the rugby players has never been
104 systematically investigated.

105 In this study, 15 retired professional and amateur rugby players (R) and 15 age-matched
106 healthy controls (HC) (all males; mean age R: 46.8 ± 7.6 ; and HC: 48.6 ± 9.5) were recruited
107 both to investigate cord impairments and further characterize brain structure damage. Medical
108 questionnaires including modified Japanese Orthopedic Association scale (mJOA) and Neck
109 Disability Index (NDI) were filled by all participants. A 3T multi-parametric MR protocol
110 including conventional qualitative techniques such as T_1 -, T_2 -, and T_2^* -weighted sequences, as
111 well as state-of-the art quantitative techniques including MP2RAGE T_1 mapping and 3D
112 ihMT-RAGE, was used on both brain and cSC. Normalized brain WM and GM volumes,
113 spine Overall Stenosis Score, cord cross-sectional area and regional T_1 and ihMT metrics
114 were derived from these acquisitions.

115 Rugby players showed significantly higher NDI scores, as well as a faster decline of
116 normalized brain GM volume with age as compared to HC. Moreover, higher T_1 values on
117 cSC suggestive of structural degeneration, together with higher T_1 and lower ihMTsat on
118 brain WM suggestive of demyelination, were observed in retired rugby players as compared
119 to age-matched controls, which may suggest cumulative effects of long-term impacts on the
120 tissues. Metrics also suggest early aging and different aging processes on brain tissue in the
121 players.

122 These preliminary observations provide new insights in the domain, which should now be
123 further investigated on larger cohorts and multicentric longitudinal studies, and further
124 correlated to the likelihood of neurodegenerative diseases and risk factors.

125

126 **Keywords**

127 Rugby, Brain, Cervical spinal cord, T_1 MP2RAGE, inhomogeneous Magnetization Transfer,
128 Neurodegeneration.

129

1 Introduction

130

131 Players of contact sports, such as rugby, receive repetitive impacts to their head and neck that
132 do not necessarily result in observable injuries ¹. However, there have been several studies
133 demonstrating the adverse effects of these impacts on the health of players. Most of these
134 studies, focusing on the brain, demonstrated that rugby players, even without a history of
135 concussion, may present lower visuomotor processing speed ², more cognitive vulnerability ³
136 and longer reaction times ⁴ compared to age-matched controls. Diffusion Tensor Imaging
137 (DTI) and functional MRI (fMRI) studies on brain have also demonstrated impaired
138 microstructure with decreased Fractional Anisotropy (FA) in multiple white matter (WM)
139 tracts accompanied with default mode network and visual network hyperconnectivity in
140 rugby players in-season as compared to off-season, which was not observed in players of
141 non-contact sports ⁵. On spine, rugby players were found to have more chronic neck pain and
142 foraminal stenosis, narrower vertebral canal, and more substantial osteophytes as compared
143 to age-matched healthy controls ^{6,7}. However, no studies have been conducted so far to
144 characterize potential effects on the cervical spinal cord (cSC) itself.

145 In this study, we propose to use complementary state-of-the-art quantitative MRI techniques
146 that have been recently adapted to brain and SC imaging at 3 T to scan retired rugby players
147 that have played in amateur and professional leagues. The protocol included a fast 3D
148 Magnetization Prepared 2 Rapid Acquisition Gradient Echo (MP2RAGE) T₁ mapping of both
149 brain and cervical cord ⁸, as well as the recent 3D inhomogeneous Magnetization Transfer
150 with rapid acquisition gradient echo technique (ihMTRAGE) ⁹. Conventional T₁ relaxometry
151 has already been used widely to study tissue alterations in pathologies such as Multiple
152 Sclerosis (MS) or Parkinson's disease (PD) ¹⁰⁻¹², where it was demonstrated to be sensitive to
153 demyelination, iron deposition or structural variations. Interestingly demyelination and iron
154 accumulation could affect T₁ in opposite directions ¹³, T₁ could therefore lack specificity if
155 both phenomena are present. The ihMT method, on the other hand, is more specific to myelin
156 in central nervous system (CNS) tissues ¹⁴⁻¹⁷. It has been used in several clinical and
157 preclinical studies on brain ^{14,16,18-23} and recently adapted to SC imaging to study
158 demyelinating pathologies such as MS and normal aging ²⁴⁻²⁷.

159 By comparing brain and cSC T₁ and ihMT metrics collected on both retired players and age-
160 matched healthy controls, this work investigated whether the cord is impaired and early tissue

161 aging occurs in the rugby player population, while refining previously reported brain tissue
162 structure damage description.

163 **2 Materials & Methods**

164 **2.1 Subjects and clinical assessments**

165 Fifteen retired rugby players (all males; 7 professionals and 8 amateurs) without known
166 neurodegenerative disease and with no prior cervical spine surgery were enrolled in the study,
167 together with 15 aged- and sex-matched healthy controls. Demographic data are summarized
168 in Table 2. The local ethics committee of our institution approved the protocol and written
169 informed consent was obtained from each participant.

170 Modified Japanese Orthopedic Association score (mJOA)²⁸ and neck pain (Neck Disability
171 Index (NDI)²⁹ questionnaires were filled by the participants to evaluate motor and sensory
172 dysfunction.

173 **2.2 MR protocol**

174 The subjects were scanned with a multi-parametric MR protocol using a 3T MR system
175 (MAGNETOM Vida, Siemens Healthcare, Erlangen, Germany) with a 20-channel head and
176 neck coil. Neck and brachial plexus MRI pads (Sat Pad Clinical Imaging Solutions, West
177 Chester, PA, USA) were installed around the subject neck and shoulders to reduce the B_0
178 magnetic field inhomogeneity. When possible for the subject, the RF coil was tilted to place
179 the cord as straight as possible and hence minimize partial volume effects (PVE) encountered
180 with non-isotropic sequences due to the cord curvature.

181 The multi-parametric MRI protocol included conventional anatomical techniques, as well as
182 quantitative MP2RAGE⁸ and ihMTRAGE⁹ sequences, as detailed in Table 1. T_2^* and ihMT
183 slices were placed perpendicular to the cord to minimize PVE. The MP2RAGE and ihMT
184 techniques are detailed in the following sections. The protocol also included a B_1^+ map
185 acquired using a pre-saturated turbo flash (TFL) sequence³⁰ to correct quantitative T_1 values
186 and ihMT signal from B_1^+ inhomogeneities (see below). The whole protocol lasted 50
187 minutes.

188

189

Sequence	Region	Orientation	Resolution (mm ³)	TR (s)	FOV (mm ²)	Acq. Time (min)	Information / MR metrics of interest
T_{2w} TSE	SC	SAG	0.6×0.6×3	3500	220×220	1:47	Disc protrusion
T_{2w}	SC	SAG	0.6×0.6×1	1500	256×256	2:42	Antero-posterior and right-

SPACE							left diameter of cord and canal; Foraminal stenosis
T₂*w MGE	SC	TRA	0.4×0.4×5	1400	180×180	5:04	GM, WM, and SC CSA
T₂w FLAIR	Brain	TRA	0.9×0.9×5	10000	240×180	2:42	Investigating (lack of) major brain abnormalities
Presat TFL	SC+Brain	SAG	5×5×5	5000	320×320	10 s	B ₁ ⁺ map used to correct T ₁ and ihMT-bias
ihMT RAGE	SC	TRA	0.9×0.9×10	2500	180×180	9:47	ihMTsat maps
	Brain		2×2×2		256×200	13:34	
	Specific parameters Low Duty Cycle (DC) high RF power ihMT preparation: train of ten 5ms-pulses (Tukey-shaped pulses with a cosine fraction of r=0.2 ³¹ ; B ₁ -peak=14.13 μT; Cosine-modulated pulses for the dual-offset saturation ^{9,21} ; repeated every 100ms (DC=5%); total saturation time 1s; B ₁ -RMS=2.95 μT; frequency offset (f) 7 kHz. Five volumes on brain: M0, MT+, MT±, MT-, MT± and 13 volumes on SC: M0+3 repetitions of (MT+, MT±, MT-, MT±).						
MP2RAGE	Brain+SC (single acquisition)	SAG	0.9×0.9×0.9	6.2	315×258	8:02	T ₁ quantitative maps; Normalized GM/WM volume
	Specific parameters T11/T12/α ₁ /α ₂ =650 ms/3150 ms/5°/3°; GRAPPA=2; Partial Fourier=6/8 ; MP2RAGE TR 4000 ms						

190 *Table 1: Multi-parametric MR protocol used for the study and derived metrics. TSE: Turbo Spin Echo; SPACE:*
191 *Sampling Perfection with Application-optimized Contrasts using different flip angle Evolution (Siemens); MGE:*
192 *Multi Gradient Echo; FLAIR: FLuid-Attenuated Inversion Recovery; CSA: Cross-Sectional Area; GM: Gray*
193 *Matter; WM: White Matter.*

194 **2.2.1 Magnetization Prepared 2 Rapid Acquisition Gradient Echo**

195 MP2RAGE is an Inversion Recovery (IR)-based technique that acquires two RAGE volumes
196 in an interleaved manner, from which a uniform (UNI) image is derived, which can then be
197 used to estimate the T₁ of the tissue voxel-wise. Originally proposed for the brain³² and
198 widely used to study pathologies like MS³³⁻³⁶, this technique was then optimized to study
199 healthy and pathological cervical cord³⁷⁻⁴⁰. Recently tuned at 3T with regards to CNR and
200 B₁⁺ insensitivity to study both brain and cSC simultaneously⁸, this latter setup was used in
201 the present study. Potential T₁ imperfections due to residual B₁⁺ inhomogeneities were
202 corrected using a B₁⁺ map as in³⁷.

203

204 **2.2.2 Inhomogeneous Magnetization Transfer**

205 IhMT has recently been proposed and validated as a myelin sensitive and specific technique
206¹⁴⁻¹⁷. The ihMT image is generated by the subtraction of a MT weighted image acquired with
207 a single frequency irradiation (MT_{sing}) and one acquired with power evenly split between
208 positive and negative frequency offsets (MT_±)²⁴. In practice, to limit the effects of MT
209 asymmetry⁴¹, the single frequency image MT_{sing} is obtained by adding an image at the
210 positive frequency (MT₊) and one at the negative frequency (MT₋) such that

211 $MT_{\text{sing}}=MT_{+}+MT_{-}$. Hence, for consistency, the dual offset image is acquired twice such that
212 the ihMT image is given by $ihMT=(MT_{+}+MT_{-}-2MT_{\pm})$.

213 Several variants of the ihMT technique have been proposed in the past, including single slice
214 2D ihMT-HASTE (Half-Fourier Acquisition Single-shot Turbo spin Echo) for brain¹⁵ and
215 SC²⁴⁻²⁶; 3D ihMT-GRE for brain¹⁹ and multi-slice ihMT SE-EPI for SC^{27,42}. In this study,
216 a 3D ihMTRAGE sequence initially proposed for brain⁹, and recently adapted to cervical
217 spinal cord imaging^{43,44} was used. The preparation scheme (Table 1) was similar to^{9,21} and
218 used identically for both the brain and SC. Note however, that the spatial resolution and the
219 number of repetitions differed. IhMTsat metrics, corrected for T_1 -relaxation and B_1^+ -
220 inhomogeneities that can bias regular ihMTR values (with ihMTR defined as $ihMT/2M_0$) at
221 $3T$ ^{44,45}, were derived based on a strategy recently customized for the ihMTRAGE framework
222 ²¹ (see 2.4 section).

223

224 **2.3 Morphological measurements**

225 Discal cross-sectional areas, as well as antero-posterior and right-left diameters of canal and
226 cord were manually measured by an experienced neurosurgeon for each subject using the
227 Horos software (horosproject.org), based on T_2 SPACE image (intra-rater reproducibility:
228 3.6%, 4.6%, 5.1%, 4.0%, 5.8%, and 7.6%, for canal AP diameter, canal RL diameter, SC AP
229 diameter, SC RL diameter, canal CSA, and SC CSA, respectively). Cord-to-canal (CCR) and
230 canal occupation (COR) ratios were subsequently derived (see definition in Table S1). The
231 degree of stenosis (see definition in Table 2) was assessed in the meantime using the same
232 contrast.

233 The axial T_2^* -weighted MGE images were used for the automatic segmentation of GM, WM,
234 and SC using the SCT⁴⁶ *deepseg* tool, from which mean CSAs were estimated at each level.

235 Finally, the UNI image (derived from MP2RAGE technique) was brain-extracted and
236 segmented into GM, WM, and cerebrospinal fluid (CSF) using SPM12
237 (<https://fil.ion.ucl.ac.uk/spm>) “*New segment*” tool⁴⁷. The volumes of brain GM and WM
238 were each normalized by the intracranial content (GM+WM+CSF) to remove inter-subject
239 differences and investigate variation with age.

240

241 **2.4 T1 and ihMTsat post-processing**

242 The post-processing steps to provide regional T₁ and ihMTsat measurements are depicted in
243 Figure 1.

244 All MT-weighted volumes (MT₊, MT₋, MT_±) of the ihMTRAGE images acquired on SC and
245 brain were motion-corrected by SCT⁴⁶ *MoCo* and *ihMT-MoCo*⁴⁸, respectively. After motion
246 correction, the MT-weighted volumes on SC and brain were registered to their respective T₁
247 maps using SCT *multi-modal registration* and SyN-ANTS⁴⁹ rigid registration tools,
248 respectively. As previously mentioned, the ihMTR ratio was not used in this study, instead
249 the ihMTsat metric was calculated. The reader can refer to Munsch et al²¹. Briefly, the
250 derivation of ihMTsat approach²¹ relies on a model that describes the effect of each RF
251 saturation pulse as a fractional attenuation (δ) of the free water pool (e.g. the free pool
252 magnetization right after a dual-offset RF pulse (MT_±') is related to the magnetization right
253 before (MT_±) by $MT_{\pm}' = (1 - \delta_{M_{\pm}}) \times MT_{\pm}$. B₁ and T₁ maps were used to determine the δ factors
254 that fit the attenuation of each MT-w relative to the unsaturated M₀ image, given the
255 ihMTRAGE sequence parameters. The ihMTsat metric was finally derived from to the
256 formulae²¹:

$$257 \quad ihMTsat = (2\delta_{MT_{\pm}} - \delta_{MT_{+}} - \delta_{MT_{-}}) \times \left(\frac{B_{1nom}}{B_{1act}} \right)^2,$$

258

259 Where the term $\left(\frac{B_{1nom}}{B_{1act}} \right)^2$ that accounts for the quadratic B₁ dependence of ihMT with the
260 saturation parameters used⁵⁰ corrects for B₁ inhomogeneities. B_{1nom} and B_{1act} represent the
261 nominal and actual pulse amplitudes calculated from the B₁⁺ map, respectively. The post-
262 processing pipeline for ihMTsat maps derivation is available in:
263 https://github.com/lsoustelle/ihmt_proc (hash f3f49e0).

264 The T_1 maps were then non-linearly registered to the ICBM-MNI-152^{51,52} template on brain
265 and PAM50 template on SC⁵³. On SC, the PAM50 regions of interest including WM
266 Corticospinal Tracts (CST), Lateral Sensory Tracts (LST), Posterior Sensory Tracts (PST),
267 Rubro/Reticulospinal Tracts (RST), and anterior and intermediate GM (ant-int) were warped
268 back into the subject space and used for quantification of the quantitative maps. On brain, in
269 addition to WM and cortical GM compartments, deep GM structures including Thalamus,
270 Nucleus Caudate, and Putamen were segmented using FSL *FIRST* tool
271 (<https://fsl.fmrib.ox.ac.uk/>)⁵⁴. The brain maps were quantified for each of these
272 compartments and deep GM regions.

273

274 **2.5 Statistical analyses**

275 The statistical analyses were performed using JMP Version 9 (SAS Institute Inc., Cary, NC).
276 The mJOA and NDI scores were compared between the rugby players and controls using the
277 non-parametric Steel-Dwass all pairs test, separately, and a p-value<0.05 was considered as
278 statistically significant.

279 For SC, T_1 and ihMTsat parameters were compared between Rugby players and healthy
280 controls using ANOVA, looking at the (R vs. HC) group effect when accounting for age and
281 cervical levels. P values were corrected for multiple comparisons (5 ROIs, 2 parameters,
282 $p_{\text{corrected}} < 0.005$).

283 For the brain, T_1 and ihMTsat parameters were also compared between Rugby players and
284 healthy controls in the three compartments using ANOVA, looking at the (R vs. HC) group
285 effect when accounting for age. P values were corrected for multiple comparisons (3
286 compartments, 2 parameters, $p_{\text{corrected}} < 0.008$).

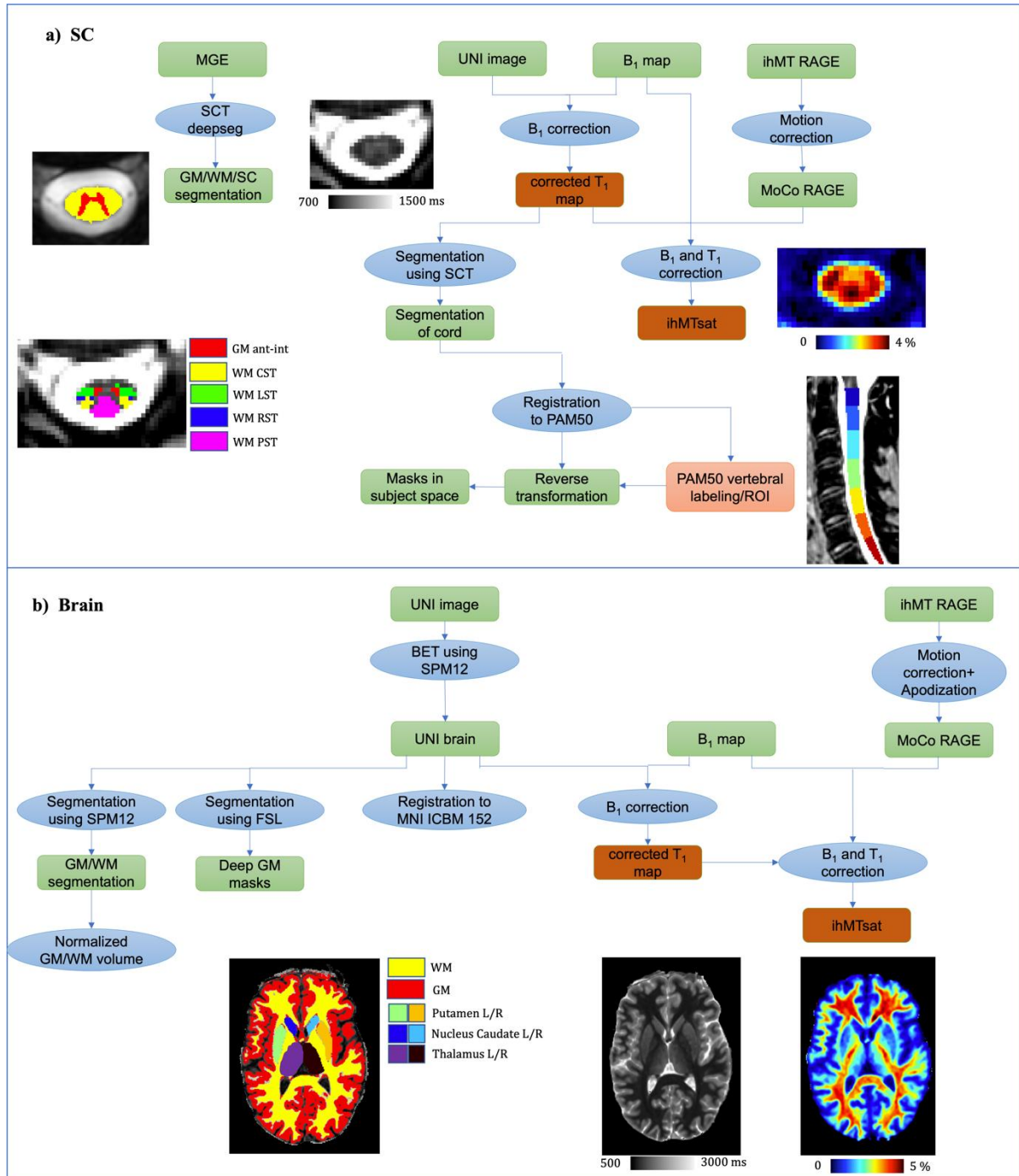
287 To investigate the evolution of metrics with age, linear regressions were performed.

288 Finally, R_1 ($1/T_1$) and ihMTsat maps on brain and SC were used in voxel-wise multi-variate
289 analyses using the Permutation Analysis of Linear Models (PALM) tool available in the FSL
290 package (version alpha119)⁵⁶. The Non-Parametric Combination (NPC) option⁵⁵, which
291 allows joint inference over multiple modalities, was more particularly used in this study. To
292 benefit from the multi-parametric MR protocol, R_1 and ihMTsat maps were thus combined
293 using NPC in order to locate potential tissue abnormalities and investigate whether R_1 and
294 ihMTsat were significantly lower in players as compared to HC. For both brain and SC, the
295 analysis was performed using WM mask, GM mask, and the whole structure. For the
296 analysis, 5000 permutations were used, along with the Threshold Free Cluster Enhancement

297 (TFCE) option. The results were corrected for Family-Wise Error (FWEP-corrected) and for
 298 multiple modalities. The threshold was then set at p-value<0.05.

299

300



301

302 *Figure 1: Main post-processing steps (motion correction, B₁⁺ and/or T₁ bias-correction, registration and*
 303 *segmentation, ROI labeling) for MP2RAGE and ihMT images on both a) SC and b) brain. (ROIs on SC: GM*
 304 *ant-int: anterior and intermediate; WM CST: corticospinal tracts; LST: lateral sensory tracts; RST:*
 305 *rubro/reticulospinal tracts; PST: posterior sensory tracts).*

306 2.6 Data/code availability statements

307 Data can be made available via a request to the authors and will be shared through a formal
308 data sharing agreement.

309 The post-processing code has been well described in the Materials & Methods section and
310 Figure 1, with all the software and toolboxes used (SCT, FSL, SPM, ANTS, etc.). The
311 ihMTsat map derivation code is also available at: https://github.com/lsoustelle/ihmt_proc
312 (hash f3f49e0)).

313 3 Results

314 3.1 Clinical assessment

315 All scores are summarized in Table 2. All rugby players and 13 HC presented at least one
316 grade of canal stenosis. NDI were significantly higher in players than in controls (p-
317 value<0.005), but with values ranging from normal to mild disability. No significant
318 differences were observed between the mJOA scores of players and HC, however, 3 amateur
319 players presented mild alterations.

320

321

	Retired Rugby Players (R)	Healthy controls (HC)
Number of participants	15	15
Players in front / second / third row position	8 / 4 / 3	-
Mean age (years old (yo)) [min, median, max]	46.8±7.6 [34, 46, 62]	48.6±9.5 [37, 47, 71]
Mean rugby practice duration (yo)	26.2±9.5	-
Mean duration from rugby practice retirement (yo)	9.8±5.4	-
Clinical scoring		
mJOA (/17)	16.7±0.5	17
NDI (%) [min, median, max]	9.4±7.2 ** [0, 8, 30]	4±8.7 [0, 0, 34]
OSS [min, median, max]	1.8±0.8 [1, 2, 3]	1.9±1.1 [0, 2, 4]
<i>mJOA, from 0 to 17, with values between 15 to 17 considered as mild degeneration and ≤ 14 as moderate-to-severe ²⁸ ; NDI, from 0 to 50; also expressed from 0 to 100%, with values <8%, < [10-28%], and [30-48%] considered as normal, mild and moderate disability, respectively ²⁹; OSS, from 0 to 18, defined as the sum of stenosis score at each level (C2-3 to C6-C7 and C1) in a range of 0 to 3 for normal, mildly, moderately, or severely compressed, respectively.</i>		

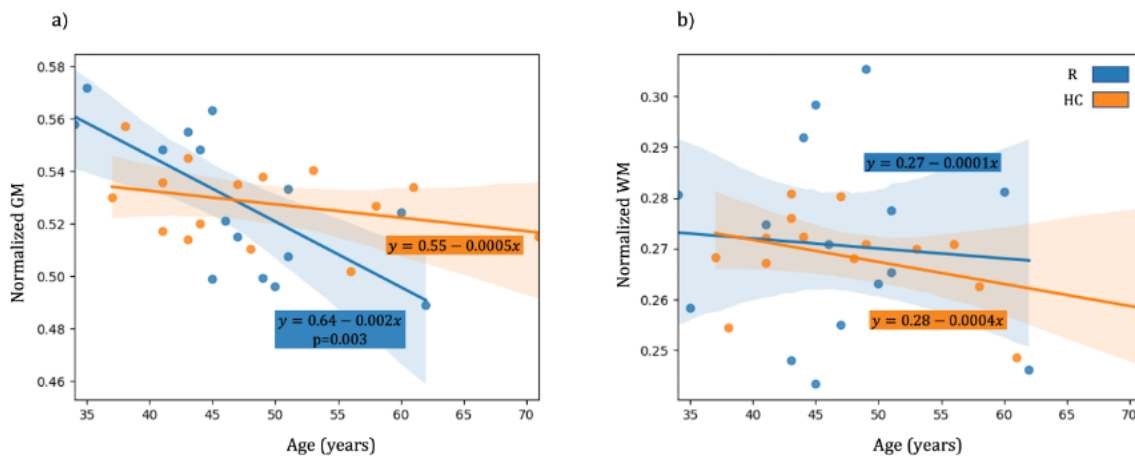
322 Table 2: Demographic data, NDI and mJOA scores, and overall stenosis score (OSS); **: p-value<0.01.

323

324 **3.2 Morphological results**

325 Morphological results are summarized in table S1 (supplementary data). No differences in SC
326 and brain morphometrics were observed between rugby players and healthy controls.
327 However, for cerebral GM compartment, one age×group interaction was observed (ANOVA
328 $p < 0.03$) related to a significant negative correlation between normalized GM volume and age
329 in rugby players ($p = 0.003$), not observed in controls. (Figure 2a).

330
331

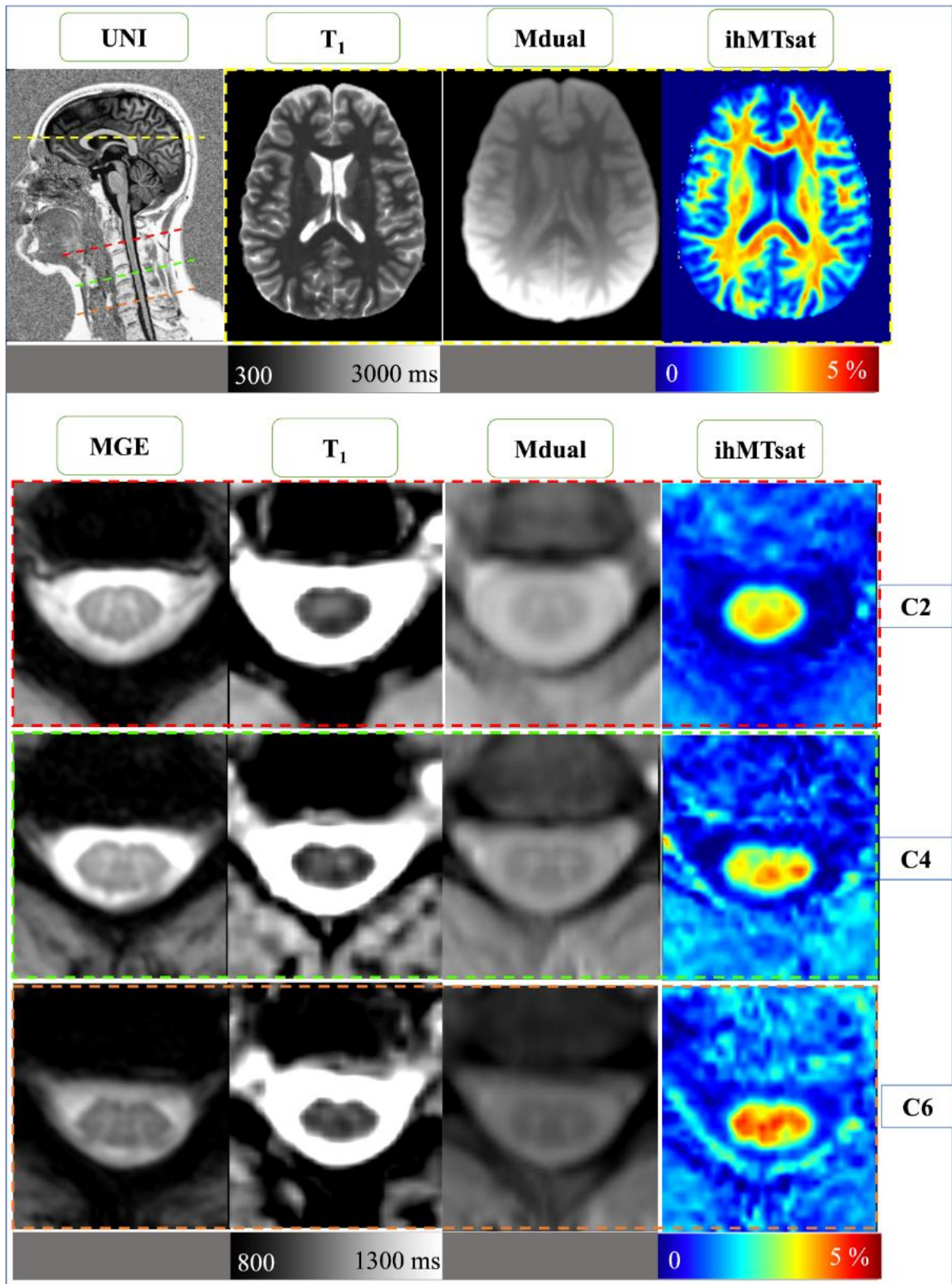


332
333 *Figure 2: Regression plots for (a) Normalized GM and (b) Normalized WM (on brain) volumes vs. age, for*
334 *Rugby players (R, blue) and Healthy Controls, (HC, orange). Age had a significant effect on the normalized GM*
335 *volume in the rugby players group ($p = 0.003$) that was not observed in HC, nor in WM.*

336

337 **3.3 Quantitative imaging results**

338 Representative images and quantitative T_1 and ihMTsat maps of both brain and SC obtained
339 from one rugby player are provided on Figure 3.



340

341 *Figure 3: Representative SC and brain images acquired on one retired rugby player (top: sagittal UNI*
 342 *MP2RAGE showing both brain and cervical cord; axial quantitative T_1 map, axial MT weighted image obtained*
 343 *with a dual-offset saturation (MT_{dual}) and corresponding ihMTsat acquired mid-brain; bottom: axial T_2^* -*
 344 *weighted MGE, T_1 map, MT_{dual} and ihMTsat acquired at C2, C4 and C6 levels).*

345

346 IhMT data biased from PVE due to cord curvature (visual assessment) were removed from
 347 the analysis (2, 2, 8, and 9 images for the C1, C2, C6, and C7 levels, respectively, for rugby
 348 players and 1, 1, 1, 7 and 8 images at C1, C2, C5, C6, and C7 levels for the HC). Brain
 349 ihMTsat maps of one rugby player and one HC were also removed because of motion
 350 artifacts. Conversely, brain and SC T_1 maps of all subjects were kept.

351 Mean maps of R_1 ($1/T_1$) and ihMTsat for both rugby players and HC groups (obtained by
 352 averaging all individual maps co-registered in the PAM50 and MNI-152 template spaces) are
 353 presented on Figure 4. Rugby players globally presented with lower R_1 (i.e. higher T_1) on SC,
 354 and a trend toward lower R_1 and ihMTsat on brain.

355 Mean T_1 and ihMTsat values in the different ROIs are summarized on table 3 for both brain
 356 and cord, and for the 2 groups. On all ROIs of SC, the T_1 values were significantly higher in
 357 players as compared to HC. No significant differences were observed on brain. Detailed
 358 values of the 2 metrics in various brain regions derived from ICBM-MNI-152 lobes atlas^{51,52}
 359 and JHU ICBM-DTI-81 WM label atlas^{57,58} are provided in Table S2 (supplementary data)
 360 for reference and readers who might be interested, but none of them reached statistical
 361 significance.

362

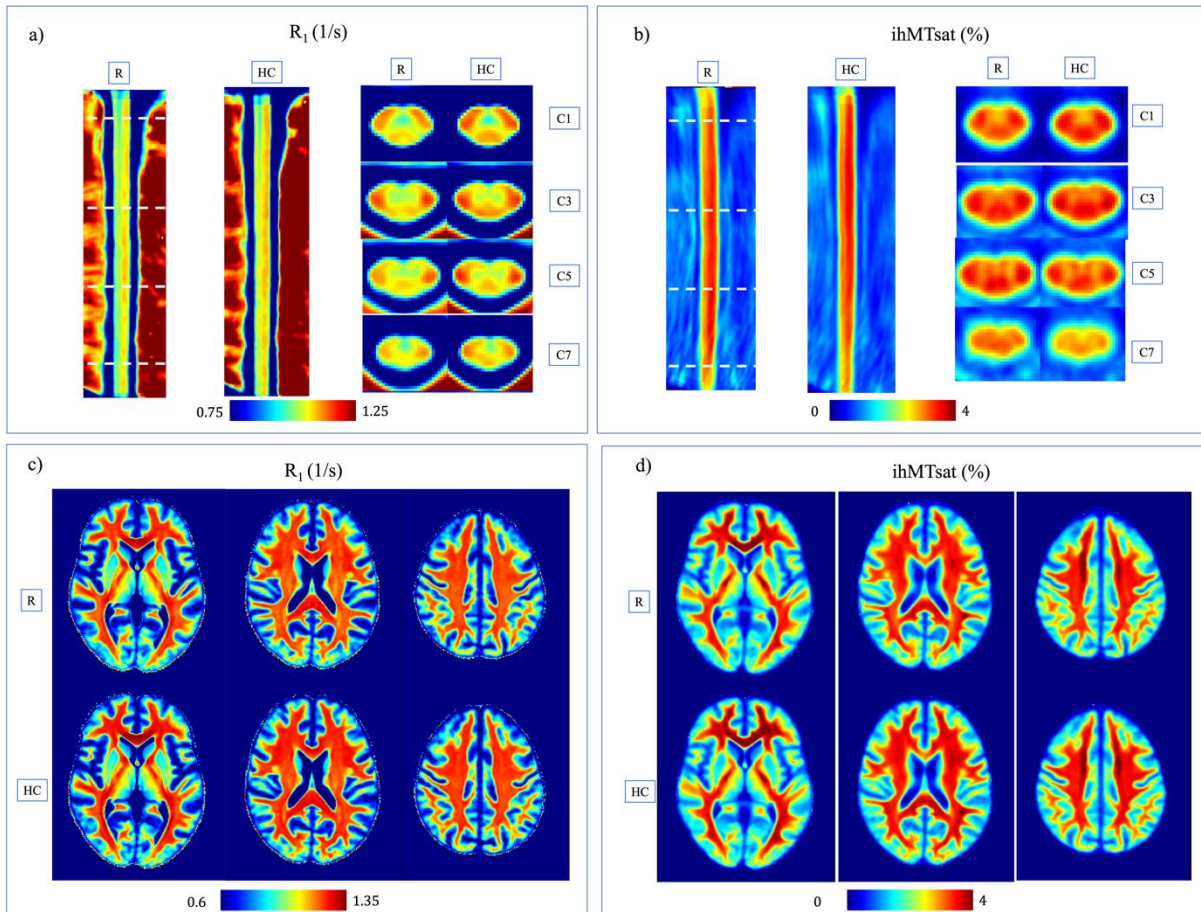
363

qMRI		T_1 (ms)		ihMTsat (%)	
SC ROI		R	HC	R	HC
WM	CST	929.7±26.5*	917.3±25.7	3.2±0.1	3.2±0.2
	PST	953.5±27.6	941.1±33	3.3±0.2	3.3±0.3
	RST	919±25.1***	901.4±25.2	3.2±0.1	3.2±0.2
	LST	925±34.2*	911.9±27.7	3.1±0.2	3.1±0.2
GM	ant-int	978.7±23.3*	967.6±19.5	3.0±0.1	3.0±0.2
Brain ROI					
WM		830.8±17.3	817.9±21.6	3.3±0.1	3.4±0.1

GM	1315.3±26.8	1307.7±19.1	1.2±0.1	1.2±0.1
dGM	1130.7±28.2	1130.1±29.7	1.4±0.1	1.4±0.1

364 Table 3: The mean \pm inter-subject SD of T_1 and ihMTsat in rugby players (R) and healthy controls (HC) in
365 different ROIs of SC and brain (see Figure 1). *: p -value<0.05, ***: p -value<0.001. The p -values correspond
366 to the MANOVA test performed on each ROI and corrected for multiple analyses (different ROIs, 2 parameters)
367 on brain and SC, separately.

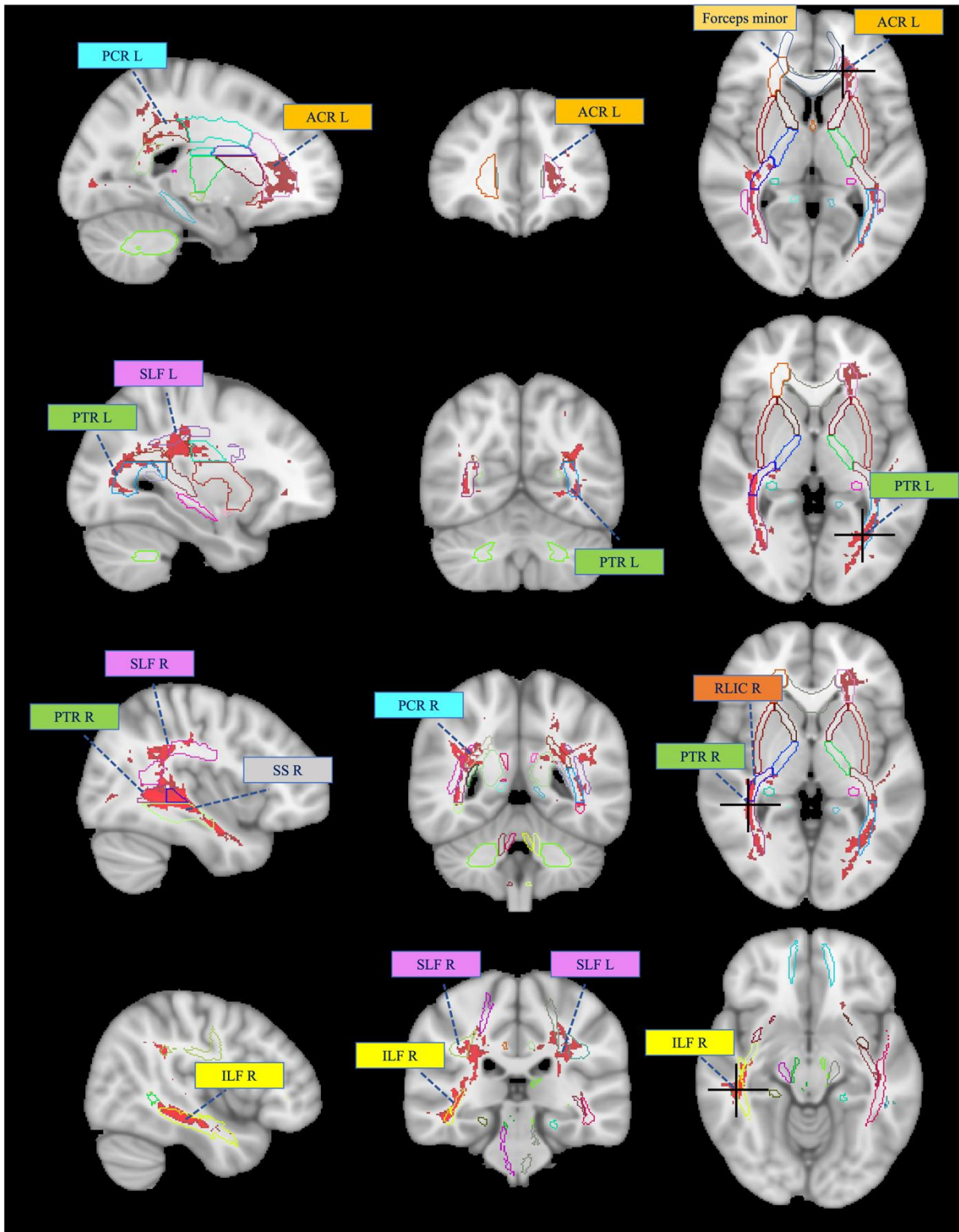
368



369 Figure 4: (a) Mean R_1 ($1/T_1$) maps on SC, (b) mean ihMTsat maps on SC, (c) mean R_1 maps on brain, (d) mean
370 ihMTsat maps on brain, for the 15 rugby players and 15 HC (sagittal and axial planes on SC, presented in the
371 PAM50 space and axial planes on brain presented in MNI-152 template).
372

373

374 Figure 5 shows the clusters obtained by the PALM multi-variate test (with R_1 and ihMTsat
375 metrics and using brain WM mask), in which a significant decrease in R_1 and/or ihMTsat was
376 observed in players as compared to controls. Labels of tracts in which the clusters are located
377 were derived from the JHU white-matter tractography⁵⁹ and ICBM-DTI-81 white-matter
378 labels atlases^{57,58}. The same tests were done with GM mask on brain, and GM and WM
379 masks on SC, but no significant clusters were found.



380

381 *Figure 5: Identification of the WM tracts where significant clusters from the PALM multi-variate analysis of R_1*
 382 *and ihMTsat are located. The atlases used for cluster localization are JHU white-matter tractography⁵⁹ and*
 383 *ICBM-DTI-81 white-matter labels atlases^{57,58}. The ROIs illustrated here are: ACR L: Anterior Corona Radiata*
 384 *L; PCR R/L: Posterior Corona Radiata Right/Left; RLIC R: Retrolenticular Limb of Internal Capsule; PTR R/L:*
 385 *Posterior Thalamic Radiation Right/Left; SLF R/L: Superior Longitudinal Fasciculus Right/left; SS R: Sagittal*
 386 *Stratum R; ILF R: Inferior Longitudinal Fasciculus Right; and Forceps minor.*

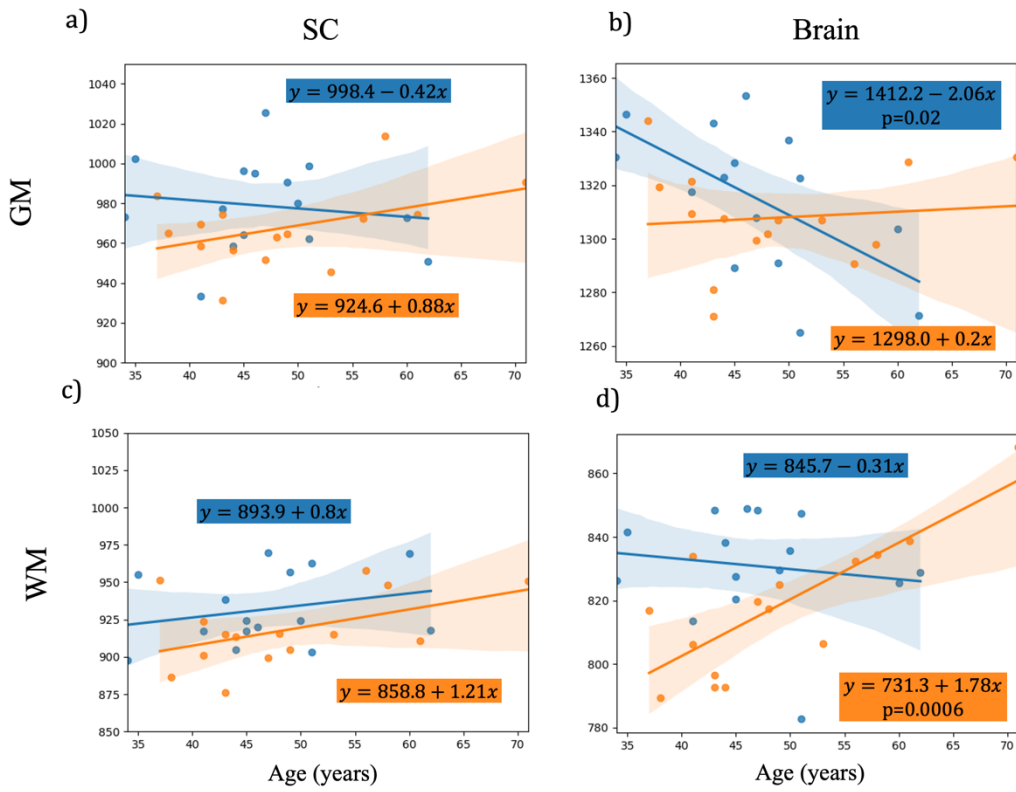
387

388

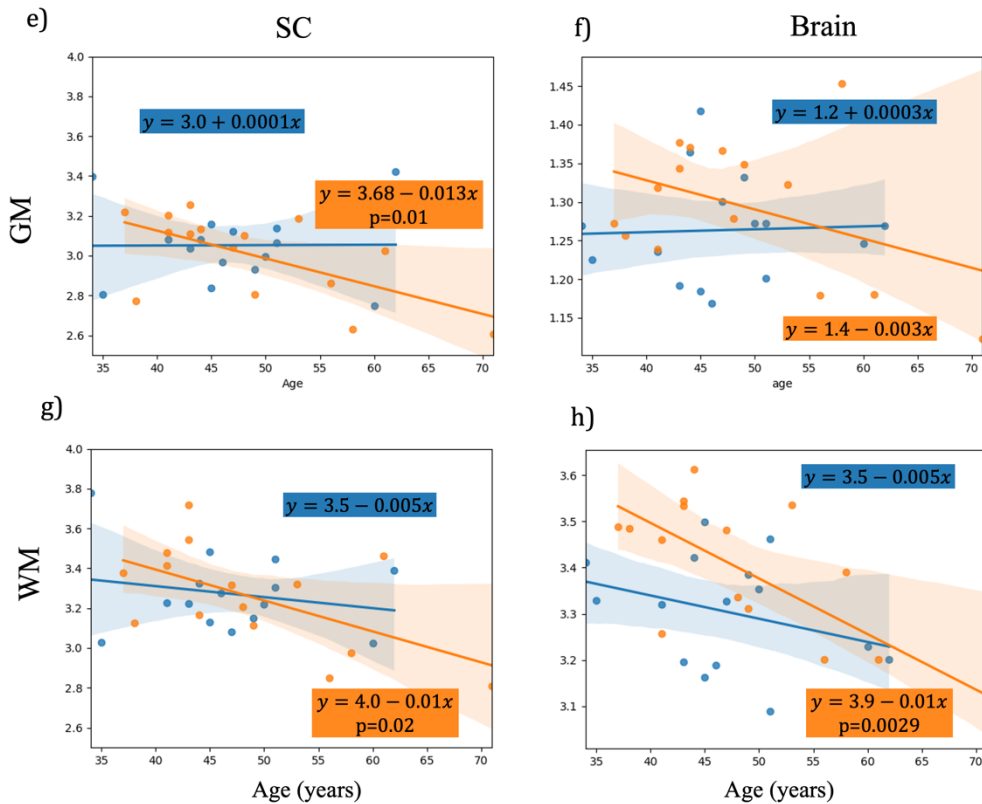
389 Finally, the linear regression plots of T_1 and ihMTsat values with age in different ROIs of
390 brain and SC are given in Figure 6. As shown from HC values (orange lines), T_1 increased
391 with age in the normal population with statistical significance in brain WM regions (Fig. 6d,
392 $p=0.0006$), and ihMTsat decreased in brain WM (Fig. 6h, $p=0.003$) and SC WM and GM
393 regions (Fig. 6e and 6g, $p\leq 0.02$). Different behaviors were observed for rugby players (blue
394 lines): T_1 decreased slightly with age in SC GM (Fig. 6a) and brain WM (Fig. 6d), and
395 significantly in brain GM (Fig. 6b, $p=0.02$), with all initial values above those of HC. For
396 ihMTsat, all initial values were below those observed in HC, values then remained fairly
397 constant with age in brain and SC GM (Fig. 6e and 6f), and slightly decreased in brain and
398 SC WM (with a slope almost divided by 2 as compared to HC, Fig. 6g and 6h).

T₁ (ms)

R ■
 HC ■



ihMTsat (%)



400 *Figure 6: Linear regression plots and equations (along with MANOVA p-value if <0.05) for evolution of T₁ and*
 401 *ihMTsat with age in GM and WM of brain and SC in R (blue) and HC (orange). The T₁ in brain and SC GM*
 402 *decreased for rugby players with age, contrary to HC (a, b). In brain WM of rugby players, a decrease of T₁*
 403 *with age together with a moderate decrease of ihMTsat as compared to HC can also be observed (d, h). Finally,*
 404 *values of ihMTsat in brain and SC GM remained fairly stable with age for rugby players whereas they tend to*
 405 *decrease for HC. GM in brain corresponds here to the whole cortical GM; WM in SC includes PST, CST, LST,*
 406 *and RST regions.*

407

408 **4 Discussion**

409

410 While spine degeneration linked to rugby activity has been previously reported ^{6,7}, little is
 411 known about the spinal cord itself. Taking advantage of a multi-parametric MR protocol
 412 including quantitative state-of-the-art T₁ MP2RAGE and ihMT techniques, both spinal cord
 413 and brain tissues from retired rugby players were analyzed in an attempt to characterize
 414 possible early aging and to refine tissue damage description. The global observations made
 415 between players and HC are summarized in Table 4. While brain and spine morphometrics
 416 were not largely affected in this population of retired rugby players, microstructure tissue
 417 damage was demonstrated, with deleterious effect of potential cumulative microtrauma
 418 highlighted with the multivariate voxel-wise approach, especially on cerebral WM tracts.

419

Metrics	Global observations	Statistical significance	Pathophysiological hypothesis / Comments
Brain qMRI			
Multi-variate analysis using R ₁ (1/T ₁) and ihMTsat in brain WM;	Lower R ₁ (higher T ₁) and lower ihMTsat for players as compared to HC, in various regions such as ACR L, PCR R/L, RLIC R, PTR R/L, SLF R/L, SS R, GCC, BCC, ILF R, and Forceps minor	p<0.05	Degeneration and demyelination in these specific WM tracts
T ₁ in GM	Significantly decreases with age in players	p=0.02	Potential iron accumulation due to micro-hemorrhages induced by repetitive impacts
T ₁ in WM	Significantly increases with age in HC but not players Initial values for players above those	p=0.0006	Early aging followed by potential iron accumulation or restructuration processes

	observed in HC		
ihMTsat in WM	Significantly decreases with age in HC but not in players Initial values for players below those observed in HC	p=0.003	Early aging followed by restructuration potentially involving microglia
SC qMRI			
Mean T ₁ in SC GM and WM	Higher T ₁ for players as compared to HC	p<0.05	Diffuse degeneration in the cord, but not necessarily due to demyelination
Mean ihMTsat in SC GM and WM	Similar range in average	No	
Clinical/Morphological assessment of Spine			
Cord-to-canal ratio (CCR)	Higher trend for players on all levels (0.62 on average)	No	Slight degenerative cervical spine (without specific cord atrophy) in the range of higher risk of trauma or chronic degenerative abnormalities ^{6,60}
NDI	Higher in players than HC, but ranging from normal to mild disability	p=0.005	Higher CCR but normal/mild disability in favor of efficient muscle strengthening programs and higher pain threshold in players ⁷

420 *Table 4: Summary of all the global observations and differences between the players and HC.*

421

422 **4.1 Clinical scoring and morphological variations**

423 Previous studies on the cervical spine of former professional rugby players showed that
424 players complained of chronic neck pain significantly more than controls, with more
425 foraminal stenosis, narrower AP cord diameter, higher CCR, but no significant difference for
426 clinical evaluations (JOA questionnaire, visual analog scale and NDI) ^{6,7}. Results from the
427 present study, performed on a much smaller cohort, globally aligned with these observations
428 (significantly higher NDI but ranging from normal to mild, slightly different AP diameter,
429 canal stenosis, and higher CCR), nonetheless spine degeneration was not prominent in this
430 population.

431 On the brain, cortical and cerebellar GM volumes were showed to reduce with age in the
432 normal population ^{61,62}. Here, the reduction in brain GM volume with age happened at a
433 significantly faster rate for rugby players, which could indicate an early aging effect in brain
434 GM linked to the rugby practice. However, the mean brain GM volume did not significantly

435 differ between players and controls, thus requiring further study on larger cohorts and time
436 points to better understand the tissue dynamic.

437

438 **4.2 Quantitative MR metrics alterations**

439 The potential microstructural alterations of the SC in players of contact sports have never
440 been studied before, except in a preliminary investigative study relying on MP2RAGE and
441 DTI that reported altered T_1 and DTI metrics in players ($n=4$), especially in levels with disc
442 protrusion⁶³. In our study and for the first time, these potential alterations were more largely
443 investigated using both T_1 and ihMTsat. The higher T_1 values in GM and WM cSC regions
444 observed in retired rugby players as compared to HC could demonstrate a diffuse
445 microstructural alteration occurring as a result of rugby practice. However, the lack of
446 difference in ihMTsat values between players and HC may indicate that the alterations are not
447 necessarily related to demyelination or that alterations seen with ihMTsat could not be caught
448 with the same sensitivity as in T_1 . Future studies should focus on the sensitivity of each
449 technique. It would also be interesting to combine MR investigation with biomechanical
450 simulations⁶³ to further understand the effects of repetitive impacts on the spinal cord tissue
451 and the presence of damage despite non prominent spine degeneration.

452 On brain, different studies have investigated the effects of sub-concussive impacts in athletes
453 of contact sports. DTI and fMRI are among the tools commonly used to study these effects
454^{5,64}. It was previously shown that football players demonstrated changes in their default mode
455 network pre-season and post-season⁶⁵, and that there was a relationship between age at first
456 exposure to football and the white matter microstructure in professional players, which
457 resulted in significant changes in DTI measures such as lower fractional anisotropy (FA) and
458 higher radial diffusivity (RD) in anterior regions of corpus callosum⁶⁴. One DTI study on ice
459 hockey players also found that axial diffusivity (AD) and RD values in the right precentral
460 region, right corona radiata, the anterior and posterior limb of the internal capsule and the
461 superior longitudinal fasciculus were significantly different pre- and post-season⁶⁶. Whereas
462 these studies demonstrate the more acute and short-term effects of alterations in players of
463 contact sports, our voxel-wise multi-variate analysis using both R_1 and ihMTsat showed
464 significant clusters in identical brain regions such as corona radiata, internal capsule, superior
465 and inferior longitudinal fasciculus, which could additionally indicate long term or persistent
466 abnormalities that may be linked to the accumulating effect of impacts encountered in the

467 rugby practice. The means of T_1 and ihMTsat in different ROIs of brain (table S2) show a
468 similar (but non-significant) trend.

469 We also observed a significant decrease of T_1 with aging in brain GM of rugby players that
470 could be indicative of excessive iron accumulation (together with a non-significant trend in
471 SC GM). Iron is essential for a normal functioning brain, however impaired regulation can
472 result in the production and accumulation of reactive oxygen species and cause oxidative
473 stress that the biological system is not able to detoxify^{67,68}. Iron accumulation occurs in brain
474 GM with normal aging^{69,70}, however, there is a growing body of evidence that repetitive
475 impacts can result in microhemorrhages and consequently, excessive iron deposition⁶⁸. In
476 parallel, excessive iron deposition has been reported in several neurodegenerative diseases
477 such as PD^{71,72}, MS⁷³, and Amyotrophic Lateral Sclerosis (ALS)^{74,75} and recent studies
478 demonstrate that contact sports that involve repetitive head and cervical spine impacts, such
479 as soccer and American football, could be a risk factor for ALS^{76,77}. Nonetheless, further
480 studies using techniques sensitive to iron such as quantitative susceptibility mapping (QSM)
481⁷⁸ would be required to further validate this hypothesis.

482 Finally, when investigating the aging effect on ihMTsat values of rugby players, we observed
483 an early decrease (in younger players as compared to HC) that could indicate demyelination
484 and early degeneration, however, values in GM and WM then did not decrease with age as in
485 HC, which may be linked to tissue restructuration involving microglia for instance⁷⁹. Indeed,
486 the ihMT technique is supposedly myelin specific, however, a recent study demonstrated that
487 ihMTsat obtained with cosine-modulated RF pulses for the dual-offset saturation (as in here)
488 is less specific to myelination than approaches using frequency-alternated RF pulses, because
489 non-myelin macromolecules, presumably associated with glial cells, also contribute to the
490 ihMTsat signal⁸⁰. Here, microglia could thus significantly contribute to the ihMTsat value,
491 hence counteracting the expected decrease of ihMTsat with age as a consequence of myelin
492 loss with age. Further studies should consider this methodological aspect to possibly
493 disentangle the different pathophysiological mechanisms.

494

495 **4.3 Limitations & Perspectives**

496 This exploratory study was performed on a retired group of rugby players and the HC group
497 was selected to match the age of players but other parameters such as profession, lifestyle, or
498 hours of sports practice were not considered. More importantly, this investigative study was
499 conducted on a limited number of participants and the effects should now be investigated in a

500 larger cohort of players. Analyses based on the players experience in professional or amateur
501 leagues could not be considered in this study due to statistical power, but similar trends were
502 observed for both sub-populations in the cohort (data not shown). This would nonetheless
503 require further investigations. The position of the players (forwards, especially front row, vs.
504 backs) could not be considered either due to statistical power, but such distinction would be
505 interesting in the future. Furthermore, a longitudinal study over time and different playing
506 seasons would allow to better delineate the short- and long-term effects of impacts.
507 Recording impacts information such as force, moment, and linear and rotational accelerations
508 as in ⁸¹⁻⁸³ would additionally enable to investigate the correlation between biomechanical
509 forces of impacts and MRI indices of structural integrity and should be considered in the
510 future.

511 Another technical limitation of this study was the spatial resolution of the ihMT technique for
512 spinal cord imaging. The slice thickness was 10 mm to maximize SNR while keeping the
513 acquisition time clinically acceptable (~10 min). This made the sequence prone to partial
514 volume effect when the cord is curved (and some data had to be discarded at the lower levels
515 of the cord) and potentially less sensitive to very focal abnormalities (which were nonetheless
516 not necessarily expected here). Note that the TR (2500 ms) could have been decreased in a
517 normal context to accelerate the acquisition time, however, the morphology of the rugby
518 players precludes such adjustment to stay within specific absorption rate (SAR) guidelines.
519 This should be further improved in future developments.

520 One should also keep in mind that the MP2RAGE technique estimates the T_1 of the tissue
521 based on the UNI image obtained from the two RAGE volumes acquired with 2 different TIs.
522 Although T_1 values obtained from MP2RAGE techniques have been previously validated in
523 phantom against IR-SE ³⁸, and against values reported in literature for different brain and SC
524 regions ⁸, it is not a pure measurement of the T_1 .

525 As mentioned in the above section, it would also be interesting to work with a frequency-
526 alternated RF pulses ihMT sequence and combine this technique with a QSM approach in
527 order to disentangle the different possible pathophysiological hypotheses that have been
528 raised in this study.

529 Despite some limitations, and to the best of our knowledge, this study is the first to
530 characterize cord tissue alterations in players of contact sports using quantitative MR
531 techniques. This study is also the first investigating both brain and cSC microstructural
532 alterations at the same time with T_1 MP2RAGE and ihMT-RAGE techniques.

533 The techniques and post-processing tools developed in this study can now be further used to
534 investigate microstructural alterations in other contact sports, different CNS pathologies or
535 aging in general.

536

537 **5 Conclusion**

538

539 In this work, retired professional and amateur rugby players and age-matched healthy
540 controls were recruited and studied for potential microstructural alterations of both brain and
541 cSC using medical questionnaires and qualitative and quantitative MR techniques including
542 T₁ relaxometry and ihMT sequences.

543 Higher NDI scores, higher cord-to-canal ratio, higher T₁ values suggestive of structural
544 degeneration of cSC, together with increased T₁ and decreased ihMTsat suggestive of brain
545 demyelination have been observed in retired rugby players as compared to age-matched
546 controls, potentially due to cumulative effect of long-term impacts. Measurements also
547 suggest early aging and different aging processes on brain in the players. These preliminary
548 observations provide new insights, which should now be further investigated on larger
549 cohorts and multicentric longitudinal studies and further correlated to the likelihood of
550 neurodegenerative diseases^{68,71-75} and risk factors.

551

552 **Acknowledgements**

553 This work was performed within a laboratory member of France Life Imaging network (grant
554 ANR-11-INBS-0006) and was supported by the Institut Carnot Star, the ARSEP Foundation
555 (Fondation pour l'Aide à la Recherche sur la Sclérose en Plaques) and the CNRS (Centre
556 National de la Recherche Scientifique). The project also received funding from the European
557 Union's Horizon 2020 research and innovation program under the Marie Skłodowska-Curie
558 grant agreement No713750, with the financial support of the Regional Council of Provence-
559 Alpes-Côte d'Azur and A*MIDEX (n° ANR-11-IDEX-0001-02), funded by the
560 Investissements d'Avenir project funded by the French Government, managed by the French
561 National Research Agency (ANR).

562 The authors would like to thank T. Kober from Siemens Healthcare for MP2RAGE sequence
563 support, A. Massire for T₁ post-processing code support, as well as V. Gimenez, C. Costes, P
564 Viout, L. Pini and MP. Ranjeva for study logistics.

565

566

MORPHOLOGICAL DATA ON BOTH SPINAL CORD & BRAIN											
Spinal cord	CCR		COR		Vertebral level	CSA (mm ²)					
	R	HC	R	HC		SC		GM		WM	
Discal level	R	HC	R	HC	Vertebral level	R	HC	R	HC	R	HC
C1	0.53±0.05	0.50±0.06	0.28±0.05	0.25±0.03	C1	76.4±5.6	77.2±8.1	15.7±1.5	15.3±1.5	60.7±4.3	61.8±7.1
C2-C3	0.66±0.06	0.64±0.07	0.37±0.06	0.34±0.03	C2	76.2±5.7	76.5±8.4	15.0±1.0	14.5±1.2	61.3±5.2	61.9±7.4
C3-C4	0.65±0.07	0.64±0.07	0.44±0.07	0.45±0.06	C3	76.2±6.4	76.4±8.7	15.3±1.6	15.6±1.2	60.9±4.9	60.8±7.7
C4-C5	0.63±0.07	0.61±0.06	0.45±0.07	0.44±0.06	C4	81.1±6.5	79.3±8.6	17.8±1.9	18.2±2.1	63.3±5.4	61.1±6.8
C5-C6	0.64±0.07	0.62±0.07	0.47±0.05	0.48±0.07	C5	78.7±7.4	77.4±11.2	17.2±2.3	17.6±2.3	61.4±5.6	59.8±9.1
C6-C7	0.61±0.09	0.60±0.06	0.41±0.08	0.43±0.05	C6	69.2±5.4	70.9±12.4	15.5±1.9	15.6±3.3	53.7±4.3	55.3±10.0
-	-	-	-	-	C7	58.1±6.5	59.4±12.8	12.4±1.8	11.0±3.8	44.9±7.2	47.2±13.7
Mean±SD	0.62±0.08	0.60±0.08	0.40±0.09	0.40±0.09	Mean±SD	73.7±9.4	73.9±11.8	15.5±2.3	15.4±3.2	58.0±8.0	58.3±10.2
Brain	Normalized GM (%)				Normalized WM (%)						
	R		HC		R		HC				
Mean±SD	52.8±1.4		52.8±2.7		26.7±0.9		27.0±1.8				

569 Table S1: Morphological measurements (mean ± inter-subject SD) on SC and brain for rugby players (R) and
570 HC: cord-to-canal ratio ($CCR = \frac{\varnothing_{AP_SC}}{\varnothing_{AP_canal}}$), canal occupation ratio ($COR = \frac{dCSA_{SC}}{dCSA_{canal}}$) and cord
571 cross sectional area (CSA), with \varnothing_{AP_SC} and \varnothing_{AP_canal} the antero-posterior (AP) diameters of cord and canal,
572 respectively, and $dCSA_{canal}$ and $dCSA_{SC}$, the canal and cord cross-sectional areas measured at each discal level
573 (C2-3 to C6-7 and C1 vertebral level). Discal cross-sectional areas and right-left (RL) or AP diameters are not
574 reported here but could be provided upon request. No statistical differences were observed between rugby
575 players and healthy controls except for \varnothing_{AP_canal} on C2-C3 (R vs. HC: 12.0±0.9 mm vs. 12.8±1.2 mm; p-
576 value<0.05) and \varnothing_{RL_canal} on C1 (R vs. HC: 22.5±2.2 mm vs. 24.3±1.8 mm; p-value<0.05).

577

578

QUANTITATIVE DATA ON SPECIFIC AREAS OF THE BRAIN					
Brain ROI		T1 (ms)		ihMTsat (%)	
		R	HC	R	HC
GM	Frontal	1285.3±32.8	1279.3±23.2	1.4±0.1	1.4±0.1
	Parietal	1269.1±30.9	1262.7±22.3	1.3±0.1	1.3±0.1

	Occipital	1283.4±30.1	1277.9±20.9	1.2±0.1	1.2±0.1
	Temporal	1388.8±34.8	1379.6±22.8	1.2±0.1	1.2±0.1
dGM	Thalamus	1195.7±30.3	1200.3±32.8	1.1±0.1	1.1±0.1
	Putamen	1142.1±31.3	1139.9±28.4	1.3±0.1	1.4±0.1
	Nucleus Caudate	1054.3±25	1049.9±36.8	1.8±0.1	1.8±0.1
WM Tracts	Corpus Callosum (CC) Genu	790.7±16.7	777.9±23	3.5±0.5	3.7±0.2
	CC Body	813.5±15.9	800.8±20.9	3.1±0.4	3.3±0.1
	CST	903.9±17.2	900.7±21	3.3±0.2	3.3±0.2
	Retrolenticular part of internal capsule R	811.2±20.8	794.9±20.9	3.1±0.4	3.4±0.2
	Anterior Corona Radiata R / L	818.3±21.3/ 816.9±20.9	800.1±24.8/ 798.8±24.1	3.4±0.5/ 3.4±0.4	3.6±0.2/ 3.7±0.1
	Posterior Corona Radiata R / L	845±19.2/ 846.7±16.6	823.4±32.7/ 825.3±30.8	3±0.4/ 3.1±0.4	3.3±0.2/ 3.4±0.2
	Posterior Thalamic Radiation R/ L	822.4±23.3/ 817.9±20.8	796.9±33.5/ 794±30.7	3.2±0.4/ 3.2±0.4	3.4±0.2/ 3.6±0.2
	Sagittal Stratum R/ L	832±20.8/ 837.4±17.7	806.9±23/ 819±22.9	3±0.4/3.1±0.4	3.3±0.2/ 3.2±0.2
	External Capsule R/L	848.4±22.2/846.9±21.7	832.3±22.3/832±21.7	3.1±0.1/3.1±0.4	3.2±0.1/3.3±0.1
	Cingulate Gyrus R/ L	804.3±20.1/797.6±18.8	790.7±22.1/784.4±20.4	3±0.4/ 3.1±0.4	3.2±0.1/ 3.2±0.2
	Fornix R	827.8±23.6	818.9±23.7	2.7±0.3	2.9±0.1
	Tapetum R / L	877.2±34.1/867.7±30.4	843.9±28/ 837.3±24.6	2.5±0.4/ 2.5±0.4	2.7±0.2/ 2.8±0.2

579

580 *Table S2: Mean±SD (inter-subject) for T₁ and ihMTsat in different brain WM and GM ROIs for rugby players*

581 *(R) and healthy controls (HC). No statistical differences could be observed, although some ROIs presented a*

582 *trend for higher T₁ and lower ihMTsat for rugby players, also seen on Figure 4.*

583

584

585

586

587

588

589 **References**

590

- 591 1. Bathgate A, Best JP, Craig G, Jamieson M. A prospective study of injuries to elite
592 Australian rugby union players. *Br J Sports Med.* 2002;36(4):265-269.
593 doi:10.1136/bjism.36.4.265
- 594 2. Shuttleworth-Rdwards AB, Radloff SE. Compromised visuomotor processing speed in
595 players of Rugby Union from school through to the national adult level. *Arch Clin*
596 *Neuropsychol.* 2008;23(5):511-520. doi:10.1016/j.acn.2008.05.002
- 597 3. Alexander DG, Shuttleworth-Edwards AB, Kidd M, Malcolm CM. Mild traumatic
598 brain injuries in early adolescent rugby players: Long-term neurocognitive and
599 academic outcomes. *Brain Inj.* 2015;29(9):1113-1125.
600 doi:10.3109/02699052.2015.1031699
- 601 4. Hume PA, Theadom A, Lewis GN, et al. A Comparison of Cognitive Function in
602 Former Rugby Union Players Compared with Former Non-Contact-Sport Players and
603 the Impact of Concussion History. *Sport Med.* 2017;47(6):1209-1220.
604 doi:10.1007/s40279-016-0608-8
- 605 5. Manning KY, Brooks JS, Dickey JP, et al. Longitudinal changes of brain
606 microstructure and function in nonconcussed female rugby players. *Neurology.*
607 2020;95(4):E402-E412. doi:10.1212/WNL.00000000000009821
- 608 6. Berge J, Marque B, Vital JM, Sénégas J, Caillé JM. Age-related changes in the
609 cervical spines of front-line rugby players. *Am J Sports Med.* 1999;27(4):422-429.
610 doi:10.1177/03635465990270040401
- 611 7. Brauge D, Delpierre C, Adam P, Sol JC, Bernard P, Roux FE. Clinical and radiological
612 cervical spine evaluation in retired professional rugby players. *J Neurosurg Spine.*
613 2015;23(5):551-557. doi:10.3171/2015.1.SPINE14594
- 614 8. Forodighasemabadi A, Rasoanandrianina H, El Mendili MM, Guye M, Callot V. An
615 optimized MP2RAGE sequence for studying both brain and cervical spinal cord in a
616 single acquisition at 3T. *Magn Reson Imaging.* 2021;84(September):18-26.
617 doi:10.1016/j.mri.2021.08.011
- 618 9. Varma G, Munsch F, Burns B, et al. Three- dimensional inhomogeneous
619 magnetization transfer with rapid gradient- echo (3D ihMTRAGE) imaging. *Magn*
620 *Reson Med.* 2020;(April):mrm.28324. doi:10.1002/mrm.28324
- 621 10. Haacke EM, Cheng NYC, House MJ, et al. Imaging iron stores in the brain using

- 622 magnetic resonance imaging. *Magn Reson Imaging*. 2005;23(1):1-25.
623 doi:10.1016/j.mri.2004.10.001
- 624 11. Sian-Hülsmann J, Mandel S, Youdim MBH, Riederer P. The relevance of iron in the
625 pathogenesis of Parkinson's disease. *J Neurochem*. 2011;118(6):939-957.
626 doi:10.1111/j.1471-4159.2010.07132.x
- 627 12. Paul F. Pathology and MRI: exploring cognitive impairment in MS. *Acta Neurol*
628 *Scand*. 2016;134(July):24-33. doi:10.1111/ane.12649
- 629 13. Stüber C, Morawski M, Schäfer A, et al. Myelin and iron concentration in the human
630 brain: A quantitative study of MRI contrast. *Neuroimage*. 2014;93(P1):95-106.
631 doi:10.1016/j.neuroimage.2014.02.026
- 632 14. Varma G, Duhamel G, De Bazelaire C, Alsop DC. Magnetization transfer from
633 inhomogeneously broadened lines: A potential marker for myelin. *Magn Reson Med*.
634 2015;73(2):614-622. doi:10.1002/mrm.25174
- 635 15. Girard OM, Prevost VH, Varma G, Cozzone PJ, Alsop DC, Duhamel G.
636 Magnetization transfer from inhomogeneously broadened lines (ihMT): Experimental
637 optimization of saturation parameters for human brain imaging at 1.5 Tesla. *Magn*
638 *Reson Med*. 2015;73(6):2111-2121. doi:10.1002/mrm.25330
- 639 16. Varma G, Girard OM, Prevost VH, Grant AK, Duhamel G, Alsop DC. Interpretation
640 of magnetization transfer from inhomogeneously broadened lines (ihMT) in tissues as
641 a dipolar order effect within motion restricted molecules. *J Magn Reson*. 2015;260:67-
642 76. doi:10.1016/j.jmr.2015.08.024
- 643 17. Duhamel G, Prevost VH, Cayre M, et al. Validating the sensitivity of inhomogeneous
644 magnetization transfer (ihMT) MRI to myelin with fluorescence microscopy.
645 *Neuroimage*. 2019;199(May):289-303. doi:10.1016/j.neuroimage.2019.05.061
- 646 18. Prevost VH, Girard OM, Mchinda S, Varma G, Alsop DC, Duhamel G. Optimization
647 of inhomogeneous magnetization transfer (ihMT) MRI contrast for preclinical studies
648 using dipolar relaxation time (T1D) filtering. *NMR Biomed*. 2017;30(6):1-13.
649 doi:10.1002/nbm.3706
- 650 19. Mchinda S, Varma G, Prevost VH, et al. Whole brain inhomogeneous magnetization
651 transfer (ihMT) imaging: Sensitivity enhancement within a steady-state gradient echo
652 sequence. *Magn Reson Med*. 2018;79(5):2607-2619. doi:10.1002/mrm.26907
- 653 20. Van Obberghen E, Mchinda S, Le Troter A, et al. Evaluation of the sensitivity of
654 inhomogeneous magnetization transfer (ihMT) MRI for multiple sclerosis. *Am J*
655 *Neuroradiol*. 2018;39(4):634-641. doi:10.3174/ajnr.A5563

- 656 21. Munsch F, Varma G, Taso M, et al. Characterization of the cortical myeloarchitecture
657 with inhomogeneous Magnetization Transfer imaging (ihMT). *Neuroimage*.
658 2020;225(October 2020):117442. doi:10.1016/j.neuroimage.2020.117442
- 659 22. Geeraert BL, Lebel RM, Mah AC, et al. A comparison of inhomogeneous
660 magnetization transfer, myelin volume fraction, and diffusion tensor imaging measures
661 in healthy children. *Neuroimage*. 2018;182(May 2017):343-350.
662 doi:10.1016/j.neuroimage.2017.09.019
- 663 23. Ercan E, Varma G, Mädler B, et al. Microstructural correlates of 3D steady-state
664 inhomogeneous magnetization transfer (ihMT) in the human brain white matter
665 assessed by myelin water imaging and diffusion tensor imaging. *Magn Reson Med*.
666 2018;80(6):2402-2414. doi:10.1002/mrm.27211
- 667 24. Girard OM, Callot V, Prevost VH, et al. Magnetization transfer from inhomogeneously
668 broadened lines (ihMT): Improved imaging strategy for spinal cord applications. *Magn
669 Reson Med*. 2017;77(2):581-591. doi:10.1002/mrm.26134
- 670 25. Taso M, Girard OM, Duhamel G, et al. Tract-specific and age-related variations of the
671 spinal cord microstructure: A multi-parametric MRI study using diffusion tensor
672 imaging (DTI) and inhomogeneous magnetization transfer (ihMT). *NMR Biomed*.
673 2016;29(6):817-832. doi:10.1002/nbm.3530
- 674 26. Rasoanandrianina H, Demortière S, Trabelsi A, et al. Sensitivity of the Inhomogeneous
675 Magnetization Transfer Imaging Technique to Spinal Cord Damage in Multiple
676 Sclerosis. *AJNR Am J Neuroradiol*. 2020;41(5):929-937. doi:10.3174/ajnr.A6554
- 677 27. Rasoanandrianina H, Duhamel G, Feiweier T, et al. Regional and structural integrity of
678 the whole cervical spinal cord using 3D-T1 MP2RAGE and multi-slice multi angle
679 DTI and ihMT sequences at 3T : preliminary investigations on age-related changes .
680 In: *Proceedings 25th Scientific Meeting, International Society for Magnetic Resonance
681 in Medicine*. ; 2017;p.0912.
- 682 28. Association JO. Japanese Orthopaedic Association assessment criteria guidelines
683 manual. *Tokyo Japanese Orthop Assoc*. 1996:46-49.
- 684 29. Vernon H, Mior S. The neck disability index: A study of reliability and validity. *J
685 Manipulative Physiol Ther*. 1991;14(7):409-415.
- 686 30. Chung S, Kim D, Breton E, Axel L. Rapid B1+ mapping using a preconditioning RF
687 pulse with turboFLASH readout. *Magn Reson Med*. 2010;64(2):439-446.
688 doi:10.1017/S1355771817000310
- 689 31. Harris FJ. On the Use of Windows for Harmonic Analysis with the Discrete Fourier

- 690 Transform. *Proc IEEE*. 1978;66(1):51-83. doi:10.1109/PROC.1978.10837
- 691 32. Marques JP, Kober T, Krueger G, van der Zwaag W, Van de Moortele PF, Gruetter R.
692 MP2RAGE, a self bias-field corrected sequence for improved segmentation and T1-
693 mapping at high field. *Neuroimage*. 2010;49(2):1271-1281.
694 doi:10.1016/j.neuroimage.2009.10.002
- 695 33. Kober T, Granziera C, Ribes D, et al. MP2RAGE multiple sclerosis magnetic
696 resonance imaging at 3 T. *Invest Radiol*. 2012;47(6):346-352.
697 doi:10.1097/RLI.0b013e31824600e9
- 698 34. Okubo G, Okada T, Yamamoto A, et al. MP2RAGE for deep gray matter measurement
699 of the brain: A comparative study with MPRAGE. *J Magn Reson Imaging*.
700 2016;43(1):55-62. doi:10.1002/jmri.24960
- 701 35. Marques JP, Gruetter R. New Developments and Applications of the MP2RAGE
702 Sequence - Focusing the Contrast and High Spatial Resolution R1 Mapping. *PLoS*
703 *One*. 2013;8(7):e69294. doi:10.1371/journal.pone.0069294
- 704 36. Simioni S, Amarù F, Bonnier G, et al. MP2RAGE provides new clinically-compatible
705 correlates of mild cognitive deficits in relapsing-remitting multiple sclerosis. *J Neurol*.
706 2014;261(8):1606-1613. doi:10.1007/s00415-014-7398-4
- 707 37. Massire A, Taso M, Besson P, Guye M, Ranjeva JP, Callot V. High-resolution multi-
708 parametric quantitative magnetic resonance imaging of the human cervical spinal cord
709 at 7T. *Neuroimage*. 2016;143:58-69. doi:10.1016/j.neuroimage.2016.08.055
- 710 38. Rasoanandrianina H, Massire A, Taso M, et al. Regional T1 mapping of the whole
711 cervical spinal cord using an optimized MP2RAGE sequence. *NMR Biomed*.
712 2019;32(11):1-17. doi:10.1002/nbm.4142
- 713 39. Demortière S, Lehmann P, Pelletier J, Audoin B, Callot V. Improved cervical cord
714 lesion detection with 3D-MP2RAGE sequence in patients with multiple sclerosis. *Am J*
715 *Neuroradiol*. 2020;41(6):1131-1134. doi:10.3174/ajnr.A6567
- 716 40. Baucher G, Rasoanandrianina H, Levy S, et al. T1 mapping for microstructural
717 assessment of the cervical spinal cord in the evaluation of patients with degenerative
718 cervical myelopathy. *Am J Neuroradiol*. 2021;42(7):1348-1357.
719 doi:10.3174/ajnr.A7157
- 720 41. Prevost VH, Girard OM, Varma G, Alsop DC, Duhamel G. Minimizing the effects of
721 magnetization transfer asymmetry on inhomogeneous magnetization transfer (ihMT) at
722 ultra-high magnetic field (11.75 T). *Magn Reson Mater Physics, Biol Med*.
723 2016;29(4):699-709. doi:10.1007/s10334-015-0523-2

- 724 42. Rangwala N, Varma G, Hackney D, Alsop DC. Quantification of myelin in the
725 cervical spinal cord using inhomogeneous magnetization transfer imaging. In:
726 *Proceedings 21st Scientific Meeting, International Society for Magnetic Resonance in*
727 *Medicine.* ; 2013:p.350.
- 728 43. Troalen T, Callot V, Varma G, Guye M, Alsop DC, Girard OM. Cervical Spine
729 inhomogeneous Magnetization Transfer (ihMT) Imaging Using ECG-Triggered 3D
730 Rapid Acquisition Gradient-Echo (ihMT-RAGE). In: *Proceedings 27th Scientific*
731 *Meeting, International Society for Magnetic Resonance in Medicine.* ; 2018:p.300.
- 732 44. Forodighasemabadi A, Troalen T, Soustelle L, Duhamel G, Girard O, Callot V.
733 Towards minimal T1 and B1 contributions in cervical spinal cord inhomogeneous
734 magnetization transfer imaging. In: *Proceedings 29th Scientific Meeting, International*
735 *Society for Magnetic Resonance in Medicine.* ; 2020:p.1175.
- 736 45. Varma G, Munsch F, Girard OM, Duhamel G, Alsop DC. An inhomogeneous
737 magnetization transfer (ihMT) quantification method robust to B1 and T1 variations
738 in magnetization prepared acquisitions. In: *Proceedings 27th Scientific Meeting,*
739 *International Society for Magnetic Resonance in Medicine.* ; 2019:p.4911.
- 740 46. De Leener B, Lévy S, Dupont SM, et al. SCT: Spinal Cord Toolbox, an open-source
741 software for processing spinal cord MRI data. *Neuroimage.* 2017;145(October
742 2016):24-43. doi:10.1016/j.neuroimage.2016.10.009
- 743 47. Ashburner J, Friston KJ. Unified segmentation. *Neuroimage.* 2005;26(3):839-851.
744 doi:10.1016/j.neuroimage.2005.02.018
- 745 48. Soustelle L, Lamy J, Le Troter A, et al. A Motion Correction Strategy for Multi-
746 Contrast based 3D parametric imaging : Application to Inhomogeneous Magnetization
747 Transfer (ihMT). *bioRxiv.* 2020. doi:10.1101/2020.09.11.292649
- 748 49. Helms G, Dathe H, Kallenberg K, Dechent P. High-resolution maps of magnetization
749 transfer with inherent correction for RF inhomogeneity and T1 relaxation obtained
750 from 3D FLASH MRI. *Magn Reson Med.* 2008;60(6):1396-1407.
751 doi:10.1002/mrm.21732
- 752 50. Varma G, Girard OM, Mchinda S, et al. Low duty-cycle pulsed irradiation reduces
753 magnetization transfer and increases the inhomogeneous magnetization transfer effect.
754 *J Magn Reson.* 2018;296:60-71. doi:10.1016/j.jmr.2018.08.004
- 755 51. Fonov V, Evans A, McKinsty R, Almlí C, Collins D. Unbiased nonlinear average age-
756 appropriate brain templates from birth to adulthood. *Neuroimage.* 2009;47:S102.
757 doi:10.1016/s1053-8119(09)70884-5

- 758 52. Fonov V, Evans AC, Botteron K, Almli CR, McKinstry RC, Collins DL. Unbiased
759 average age-appropriate atlases for pediatric studies. *Neuroimage*. 2011;54(1):313-
760 327. doi:10.1016/j.neuroimage.2010.07.033
- 761 53. De Leener B, Fonov VS, Collins DL, Callot V, Stikov N, Cohen-Adad J. PAM50:
762 Unbiased multimodal template of the brainstem and spinal cord aligned with the
763 ICBM152 space. *Neuroimage*. 2018;165(July 2017):170-179.
764 doi:10.1016/j.neuroimage.2017.10.041
- 765 54. Patenaude B, Smith SM, Kennedy DN, Jenkinson M. A Bayesian model of shape and
766 appearance for subcortical brain segmentation. *Neuroimage*. 2011;56(3):907-922.
767 doi:10.1016/j.neuroimage.2011.02.046
- 768 55. Winkler AM, Webster MA, Brooks JC, Tracey I, Smith SM, Nichols TE. Non-
769 parametric combination and related permutation tests for neuroimaging. *Hum Brain*
770 *Mapp*. 2016;37(4):1486-1511. doi:10.1002/hbm.23115
- 771 56. Winkler AM, Ridgway GR, Webster MA, Smith SM, Nichols TE. Permutation
772 inference for the general linear model. *Neuroimage*. 2014;92:381-397.
773 doi:10.1016/j.neuroimage.2014.01.060
- 774 57. Mori S, Oishi K, Jiang H, et al. Stereotaxic white matter atlas based on diffusion tensor
775 imaging in an ICBM template. *Neuroimage*. 2008;40(2):570-582.
776 doi:10.1016/j.neuroimage.2007.12.035
- 777 58. Hua K, Zhang J, Wakana S, et al. Tract probability maps in stereotaxic spaces:
778 Analyses of white matter anatomy and tract-specific quantification. *Neuroimage*.
779 2008;39(1):336-347. doi:10.1016/j.neuroimage.2007.07.053
- 780 59. Wakana S, Caprihan A, Panzenboeck MM, et al. Reproducibility of quantitative
781 tractography methods applied to cerebral white matter. *Neuroimage*. 2007;36(3):630-
782 644. doi:10.1016/j.neuroimage.2007.02.049
- 783 60. Castinel BH, Adam P, Milburn PD, et al. Epidemiology of cervical spine abnormalities
784 in asymptomatic adult professional rugby union players using static and dynamic MRI
785 protocols: 2002 to 2006. *Br J Sports Med*. 2010;44(3):194-199.
786 doi:10.1136/bjism.2007.045815
- 787 61. Taki Y, Thyreau B, Kinomura S, et al. Correlations among brain gray matter volumes,
788 age, gender, and hemisphere in healthy individuals. *PLoS One*. 2011;6(7):e22734.
789 doi:10.1371/journal.pone.0022734
- 790 62. Jäncke L, Mérillat S, Liem F, Hänggi J. Brain size, sex, and the aging brain. *Hum*
791 *Brain Mapp*. 2015;36(1):150-169. doi:10.1002/hbm.22619

- 792 63. Rasoanandrianina H. Toward the characterization of macro and micro -traumatism of
793 the human cervical spinal cord in rugby. *PhD Thesis*. 2019.
- 794 64. Stamm JM, Koerte IK, Muehlmann M, et al. Age at First Exposure to Football Is
795 Associated with Altered Corpus Callosum White Matter Microstructure in Former
796 Professional Football Players. *J Neurotrauma*. 2015;32(22):1768-1776.
797 doi:10.1089/neu.2014.3822
- 798 65. Abbas K, Shenk TE, Poole VN, et al. Alteration of default mode network in high
799 school football athletes due to repetitive subconcussive mild traumatic brain injury: A
800 resting-state functional magnetic resonance imaging study. *Brain Connect*.
801 2015;5(2):91-101. doi:10.1089/brain.2014.0279
- 802 66. Koerte IK, Kaufmann D, Hartl E, et al. A prospective study of physician-observed
803 concussion during a varsity university hockey season: white matter integrity in ice
804 hockey players. Part 3 of 4. *Neurosurg Focus*. 2012;33(6):1-7.
- 805 67. Núñez MT, Urrutia P, Mena N, Aguirre P, Tapia V, Salazar J. Iron toxicity in
806 neurodegeneration. *BioMetals*. 2012;25(4):761-776. doi:10.1007/s10534-012-9523-0
- 807 68. Daglas M, Adlard PA. The Involvement of Iron in Traumatic Brain Injury and
808 Neurodegenerative Disease. *Front Neurosci*. 2018;12(December).
809 doi:10.3389/fnins.2018.00981
- 810 69. del C. Valdés Hernández M, Ritchie S, Glatz A, et al. Brain iron deposits and lifespan
811 cognitive ability. *Age (Omaha)*. 2015;37(5). doi:10.1007/s11357-015-9837-2
- 812 70. Hagemeyer J, Geurts JJG, Zivadinov R. Brain iron accumulation in aging and
813 neurodegenerative disorders. *Expert Rev Neurother*. 2012;12(12):1467-1480.
814 doi:10.1586/ern.12.128
- 815 71. Zhang J, Zhang Y, Wang J, et al. Characterizing iron deposition in Parkinson's disease
816 using susceptibility-weighted imaging: An in vivo MR study. *Brain Res*.
817 2010;1330:124-130. doi:10.1016/j.brainres.2010.03.036
- 818 72. Barbosa JHO, Santos AC, Tumas V, et al. Quantifying brain iron deposition in patients
819 with Parkinson's disease using quantitative susceptibility mapping, R2 and R2*. *Magn
820 Reson Imaging*. 2015;33(5):559-565. doi:10.1016/j.mri.2015.02.021
- 821 73. Bergsland N, Tavazzi E, Laganà MM, et al. White Matter Tract Injury is Associated
822 with Deep Gray Matter Iron Deposition in Multiple Sclerosis. *J Neuroimaging*.
823 2017;27(1):107-113. doi:10.1111/jon.12364
- 824 74. Oshiro S, Morioka MS, Kikuchi M. Dysregulation of iron metabolism in Alzheimer's
825 disease, Parkinson's disease, and amyotrophic lateral sclerosis. *Adv Pharmacol Sci*.

- 2011;2011. doi:10.1155/2011/378278
- 827 75. Kwan JY, Jeong SY, van Gelderen P, et al. Iron accumulation in deep cortical layers
828 accounts for MRI signal abnormalities in ALS: Correlating 7 tesla MRI and pathology.
829 *PLoS One*. 2012;7(4). doi:10.1371/journal.pone.0035241
- 830 76. Blecher R, Elliott MA, Yilmaz E, et al. Contact Sports as a Risk Factor for
831 Amyotrophic Lateral Sclerosis: A Systematic Review. *Glob Spine J*. 2019;9(1):104-
832 118. doi:10.1177/2192568218813916
- 833 77. Chiò A, Calvo A, Dossena M, Ghiglione P, Mutani R, Mora G. ALS in Italian
834 professional soccer players: The risk is still present and could be soccer-specific.
835 *Amyotroph Lateral Scler*. 2009;10(4):205-209. doi:10.1080/17482960902721634
- 836 78. Mark Haacke E, Reichenbach JR, Wang Y. Susceptibility-Weighted Imaging and
837 Quantitative Susceptibility Mapping. *Brain Mapp An Encycl Ref*. 2015;1(1):161-172.
838 doi:10.1016/B978-0-12-397025-1.00019-1
- 839 79. Loane DJ, Byrnes KR. Role of Microglia in Neurotrauma. *Neurotherapeutics*.
840 2010;7(4):366-377. doi:10.1016/j.nurt.2010.07.002
- 841 80. Herten A, Soustelle L, Le Troter A, et al. T 1D - weighted ihMT imaging – Part I.
842 Isolation of long- and short- T 1D components by T 1D - filtering. *Magn Reson Med*.
843 2022;87(5):2313-2328. doi:10.1002/mrm.29139
- 844 81. King D, Hume PA, Brughelli M, Gissane C. Instrumented mouthguard acceleration
845 analyses for head impacts in amateur rugby union players over a season of matches.
846 *Am J Sports Med*. 2015;43(3):614-624. doi:10.1177/0363546514560876
- 847 82. King DA, Hume PA, Gissane C, Clark TN. Similar head impact acceleration measured
848 using instrumented ear patches in a junior rugby union team during matches in
849 comparison with other sports. *J Neurosurg Pediatr*. 2016;18(1):65-72.
850 doi:10.3171/2015.12.PEDS15605
- 851 83. Langevin TL, Antonoff D, Renodin C, et al. Head impact exposures in women's
852 collegiate rugby. *Phys Sportsmed*. 2021;49(1):68-73.
853 doi:10.1080/00913847.2020.1770568

854

855